3D Geophysical Inversion Modeling of Ground Magnetic Data at Baker Hot Springs, Washington State, USA

Jeffrey B. Witter[1], Dominique Fournier[2], William D. Schermerhorn[3], and Pete Stelling[3]

[1]Innovate Geothermal Ltd., Vancouver, British Columbia, Canada

[2]University of British Columbia, Vancouver, British Columbia, Canada

[3]Western Washington University, Bellingham, Washington, USA

Keywords

Geothermal exploration, magnetic data, inversion modeling, remanence, Baker hot springs

ABSTRACT

Ground-based magnetic survey data were geophysically modelled in 3D as part of a play fairway exploration program at Baker hot springs. A multi-step inversion method was used to address the issue of remanent magnetization in rocks of the study area. The geophysical modelling effort generated an effective susceptibility model that displays the 3D distribution and orientation of magnetization in the subsurface. Importantly, the magnetic modelling effort found that a strong, dipolar magnetic anomaly observed in the study area can be explained by a remanently magnetized body that is ~1¼ km long x ~200 m wide and extends from ~25-400 m below the surface. Geologically, this body may represent 1) an intrusion of reversely magnetized mafic rocks or 2) a magnetite-bearing fault zone. This rock body coincides spatially with Baker hot springs; the margins of this body or the fault structures within it are likely responsible for providing the permeability that gives rise to the hot springs.

1. Introduction

Located on the east flank of Mt. Baker volcano (Washington, USA), the Baker hot springs area is the subject of a U.S. Department of Energy geothermal play fairway exploration program (Norman et al., 2015). As part of this exploration program, ground-based magnetic survey data were collected on and off roads near Baker hot springs (Schermerhorn et al. 2017). The purpose of collecting these data is to help understand the distribution of lithology and rock structure in the subsurface as it pertains to permeable pathways that could facilitate or inhibit geothermal fluid flow. A map-based interpretation of the magnetic survey data and a preliminary 3D magnetic susceptibility model of the subsurface derived from the magnetic survey data are presented in Schermerhorn et al. (2017). The purpose of this paper is to describe the 3D

susceptibility modeling effort in more detail and provide an updated 3D magnetic model result for geological interpretation. This study is important to the field of geothermal exploration, in general, because some of the rock bodies in the subsurface near Baker hot springs likely exhibit magnetic remanence. Magnetic remanence arises when rocks preserve a magnetic moment oriented differently than the Earth's present day magnetic field direction. Such characteristics are commonly found in igneous rocks that form during periods of Earth history when the magnetic field is reversed. Interpretation of magnetic survey data in regions of magnetic remanence can often be difficult and/or misleading. Accurate 3D modeling of magnetized rocks can provide valuable insights about the geometry of the subsurface geology.

1.1 Background

Baker hot springs is located approximately 10 km east of the summit of Mt. Baker volcano. (Figure 1). Situated in a glacial-carved valley, much of the bedrock geology of the area is obscured by Quaternary sediment cover. Bedrock exposures on the flanks of the valley suggest the underlying bedrock stratigraphy consists of the following: older, Paleozoic rocks of the Chilliwack Group thrust on top of younger, Mesozoic rocks of the Nooksack Formation. The Chilliwack Group rocks (unit PCmv in Figure 1) are Permian in age and consist of breccia and pillow lava of basalt to basaltic andesite composition. The Nooksack Formation rocks (unit KJna in Figure 1) are early Cretaceous to middle Jurassic in age and consist of massive to laminated black argillite with some beds of lithic volcanic sandstone and minor limy siltstone/limestone (Tabor et al., 2003). The Nooksack Formation is believed to be autochthonous to the Mt. Baker area, relatively undeformed, and greater than 4 km thick (Tabor et al. 2003). This compares to the more extensively deformed Chilliwack Group rocks that, in some areas, are metamorphosed up to greenschist facies.

Considering these geological characteristics, we would expect the Nooksack Formation rocks to be weakly to non-magnetic. By contrast, the Chilliwack Group rocks could be strongly magnetic due to their mafic composition. Alternatively, greenschist facies metamorphism noted in the Chilliwack Group may have broken down magnetite leaving rocks with a weakly magnetic character.

1.2 Magnetic Data

In 2016, 93 line km of ground-based magnetic survey data were collected on the eastern and southern sides of Mt. Baker (Schermerhorn et al. 2017) Approximately 30 line km of these data lie within the study area described in this paper (Figure 1). The magnetic survey data are gridded across the entire study area (Schermerhorn et al. 2017) using a 15 m cell size (Figure 2). Note that for large portions of the study area, no magnetic survey data were collected. In these regions, the magnetic intensity shown in the gridded map has been inferred. To facilitate comparison with mapped geology, the Total Magnetic Intensity (TMI) data collected in the survey are presented with Reduction-to-Pole (RTP) applied, a process which places magnetic anomalies directly over their inferred sources (Figure 2). Magnetic data uncertainty of 1 nT was assumed for the purposes of the geophysical modelling. The Earth's magnetic field parameters at the time of the magnetic survey are I = 70.14°, D = 16.06°, and B = 54,318 nT, where I is inclination, D is declination, and B is total field strength.

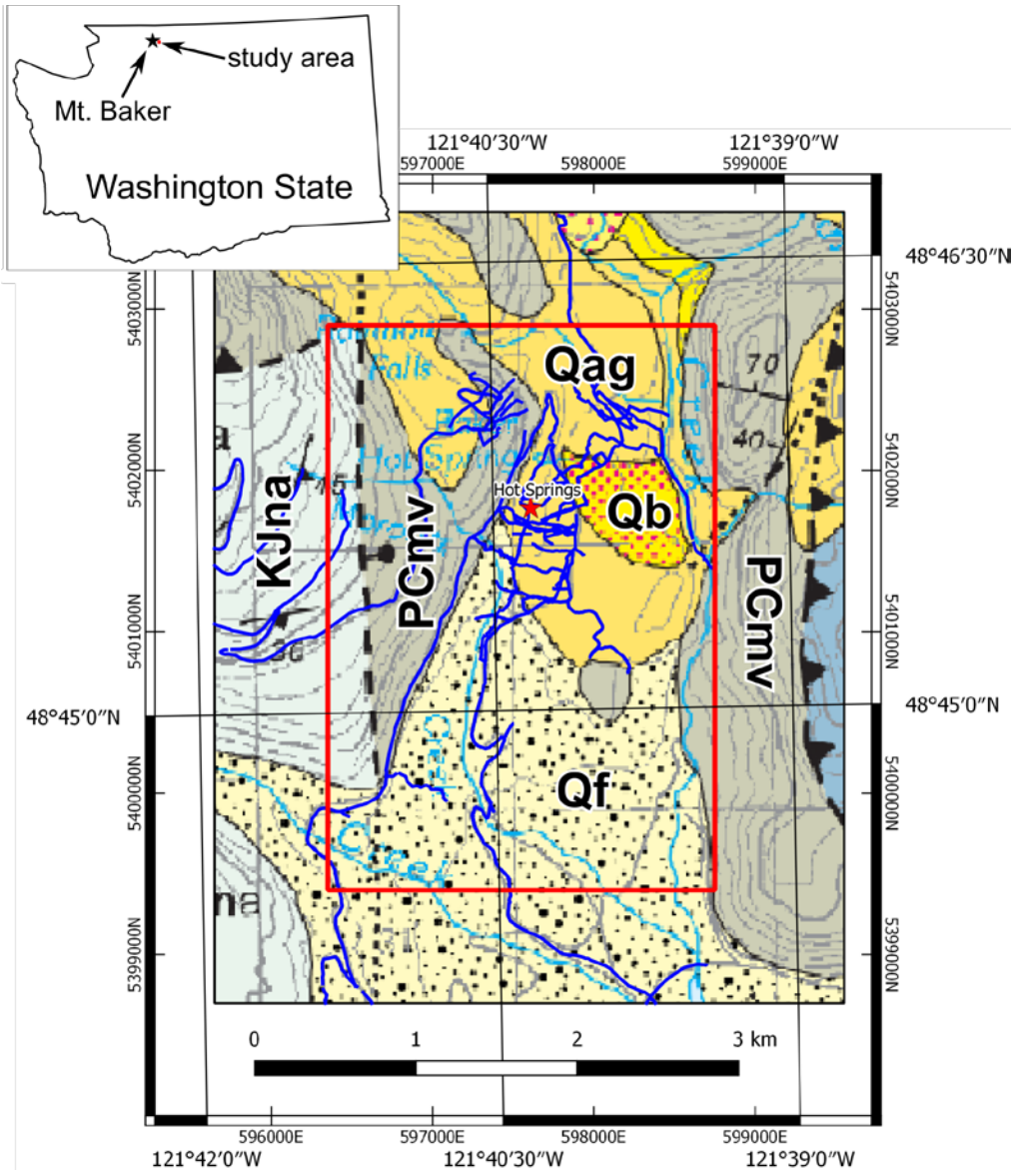

Figure 1. Geologic map of the Baker hot springs area (adapted from Tabor et al., 2003). Baker hot springs (red star), magnetic survey lines (blue), and geophysical inversion modelling area (3.5 km x 2.4 km red box) are shown. Geologic map units from youngest to oldest are as follows: Qf = Alluvial-fan deposits (Holocene), Qb = Bog deposits (Holocene), Qag = Alpine glacial deposits (Holocene and Pleistocene), KJna = Argillite and sandstone (Cretaceous-Jurassic Nooksack Formation), and PCmv = Volcanic rocks of Mount Herman (Permian Chilliwack Group). Coordinates around the map frame are shown in both latitude/longitude (WGS84) as well as UTM WGS84 zone 10 (metres). Inset map shows the location of Mt. Baker and the study area in Washington State.

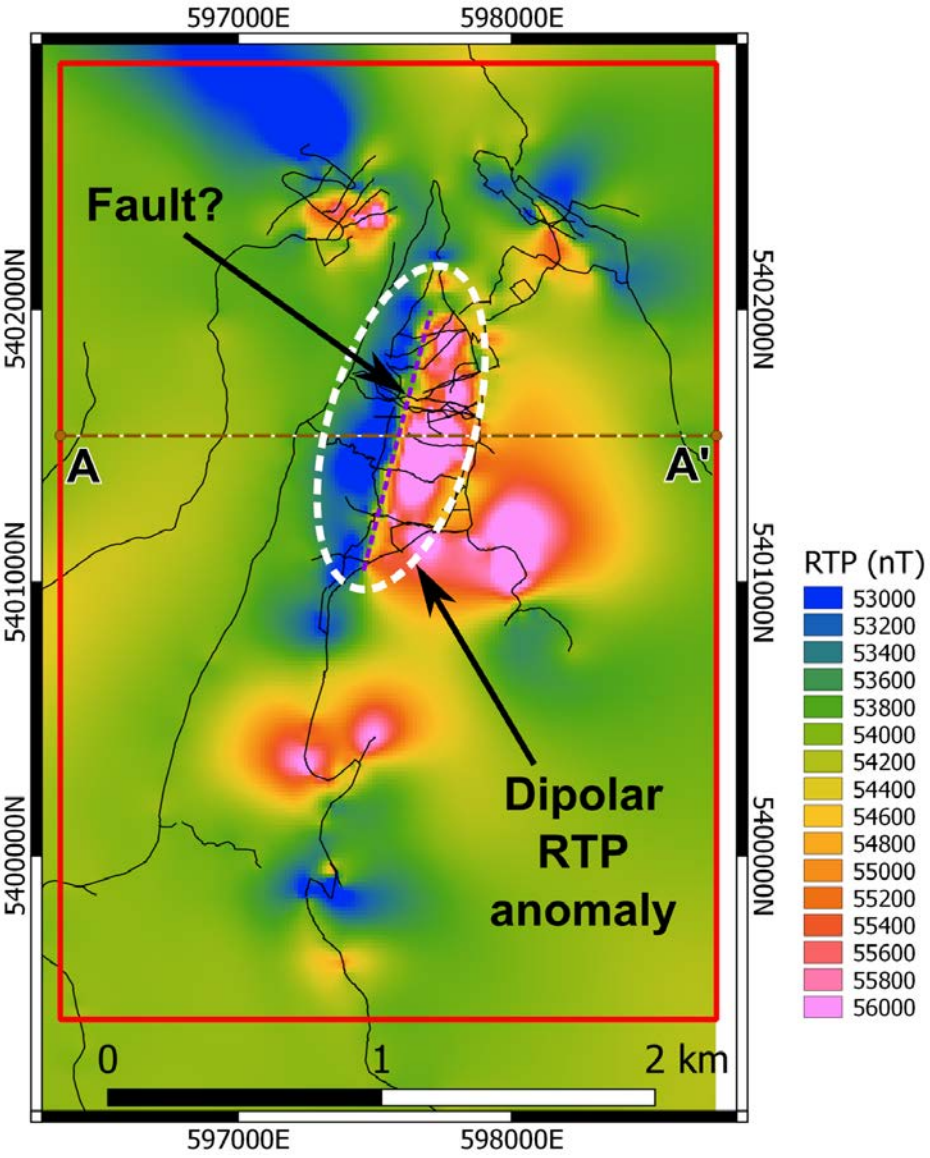

Figure 2. Reduced-to-Pole (RTP) Total Magnetic Intensity map of the Baker hot springs study area in units of nanoTesla (nT). Magnetic survey lines (black) and geophysical model area (red box) are shown. Warm colours represent regions of high magnetic intensity whereas cool colours represent low magnetic intensity. RTP magnetic anomalies do not appear to correlate with the surface geology shown in Figure 1. The study area is dominated by a strongly dipolar magnetic anomaly. Interpreted fault indicated by purple dashed line. Cross-section A-A' is shown in Figures 3 and 8.

2. Methodology

The initial 3D inversion modelling of the magnetic data was performed in an unconstrained manner and assumed no remanence. For this effort, we used the method of Li and Oldenburg, (1996).

To more accurately model magnetic remanence, we used a multi-step inversion modelling approach described in Fournier (2015). The approach is a Cooperative Magnetic Inversion algorithm (CMI) which consists of the following. In the first step, an equivalent source technique

(Li and Oldenburg, 2010; Li et al., 2014) is used on TMI data for the sole purpose of computing magnetic field amplitude data. Magnetic amplitude data are useful because they are only weakly dependent on the orientation of magnetization (Nabighian, 1972). In other words, the presence of remanently magnetized rocks does not strongly influence magnetic amplitude data. In a second step, the magnetic amplitude data are inverted (Shearer, 2005) to generate an effective susceptibility model of the subsurface. The effective susceptibility model is a semi-quantitative representation of the 3D distribution of magnetization in the subsurface. Such a model can be used to interpret the location, geometry, and relative magnetization of subsurface magnetic bodies. In a third step, the effective susceptibility model is used to constrain a Magnetic Vector Inversion (MVI) to recover the orientation of magnetization (Lelièvre, 2009).

For the purposes of the magnetic inversion modelling, the magnetic survey data were re-gridded with a 50 m cell size across the entire 2.4 km x 3.5 km study area. TMI values extracted from each of the 50 m cells were used to represent the observed magnetic field in the inversion modelling. The core of the inversion model volume (without padding cells) occupies the 2.4 km x 3.5 km study area footprint and is 2.5 km thick (from 1500 m above sea level to 1000 m below sea level). The cell size in the core model volume is 50 m x 50 m x 50 m. SRTM data were used to define the topographic surface of the model volume. In order to minimize edge effects, six padding cells of increasing size, extending a total of 800 m to the N, S, E, and W, were appended to the edges of the core model volume. In addition, nine padding cells, totaling 1200 m, were appended to the bottom of the core model volume.

The inversion modelling effort used a total of 3360 magnetic data points. The core model volume contains 168,000 cells. The model volume with padding contains 290,280 cells.

SimPEG open-source software was used for all of the geophysical inversion modelling (simpeg.xyz; Cockett et al., 2015).

3. Results

3.1 Initial Interpretation and 3D Modelling of the Magnetic Data

A comparison between the surface geology (Figure 1) and the Reduced-to-Pole magnetic map (Figure 2) reveals little correlation between rock type exposed at the surface and magnetic intensity. For example, there is no apparent contrast in magnetic intensity across the contact between Chilliwack Group rocks (PCmv) and the Nooksack Formation (KJna). Instead, the magnetic survey data is dominated by a strongly dipolar anomaly covered by Quaternary sediments, located near the north-central part of the study area (Figure 2). This anomaly is characterized by a strong magnetic low (blue) on the west and a strong magnetic high (pink) on the east. The contact between the high and low portions of this anomaly extends for ~1 km and trends NNE. One interpretation of such a magnetic anomaly is a NNE trending fault (or lithologic contact) that separates non-magnetic rocks to the west from strongly magnetic rocks to the east (Figure 2).

Following this preliminary, map-based interpretation, we performed unconstrained 3D geophysical inversion modelling to explore the 3D distribution of magnetic susceptibility in the subsurface. The TMI data were initially inverted with a coarse (100 m) cell size and magnetic remanence was assumed not present. Figure 3 shows cross-section A-A' which traverses the

dipolar magnetic anomaly near the centre of the study area (location of the section shown in Figure 2). From the magnetic data map, we would expect to recover a strongly magnetized body extending at depth to give rise to the observed, NNE-trending, dipolar anomaly. The initial 3D inversion modelling instead returned a dome-shaped zone of zero susceptibility beneath this anomaly. Magnetic inversion modelling algorithms that assume an absence of remanence, when remanence is present, often generate unreliable results (Lelièvre, 2009).

We demonstrate this point with a numerical simulation presented in Figure 4. We generate synthetic data (Figure 4a) from a simple block model consisting of a steeply dipping, 50 m wide magnetic dyke embedded in a non-magnetic background (Figure 4b). We assume that the dyke has a magnetization magnitude of 16 A/m and direction of I = 20° and D = 270°. The depth, width and magnetization direction are chosen to generate a response which resembles the observed TMI data at the study site (Figure 4a). We then proceeded with a 3D magnetic susceptibility inversion (i.e. no remanence) as presented in Figure 4c. Recovered susceptibility anomalies are shifted away from the true location of the magnetic dyke, with a dome shape zero-susceptibility feature similar to result previously shown in Figure 3. The results of this initial inversion and simulation effort suggest that magnetic remanence actually may be present in the subsurface in the Baker hot springs area. Thus, we conclude that a more advanced inversion methodology, which can account for remanence effects, is needed.

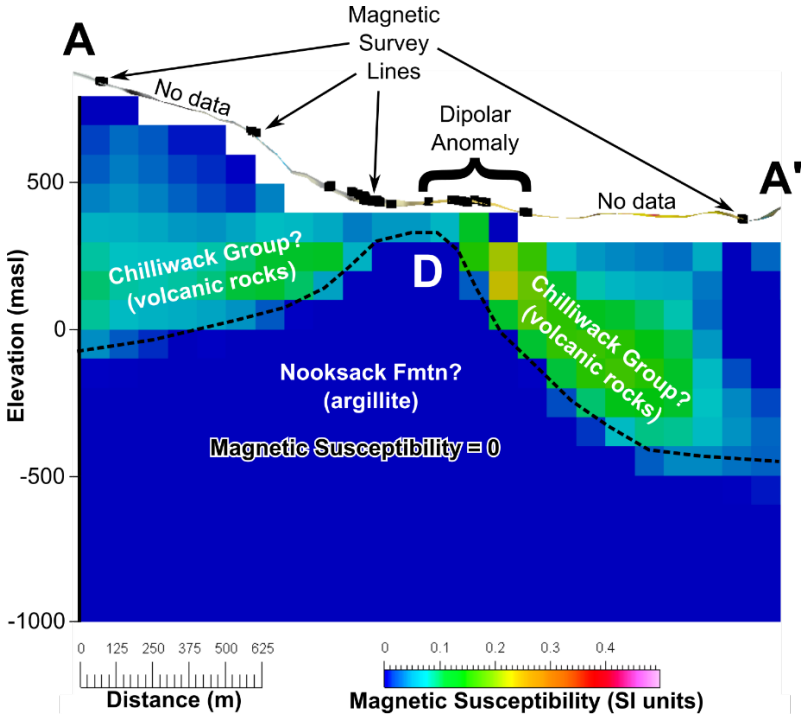

Figure 3. Section A-A' through the initial, unconstrained 3D magnetic susceptibility model (assumes no remanence). Location of section is shown in Figure 2. Section is oriented E-W and view is to the north. Warm vs. cool colours represent high vs. low magnetic susceptibility, respectively. The ribbon above the model is topography. Black squares on the topography represent the locations of the magnetic survey lines. The location where the section crosses the strong dipolar RTP anomaly is labeled. The section is also annotated with a possible geologic interpretation. The black dotted line represents the geologic contact between the Chilliwack Group and Nooksack Formation rocks inferred from this susceptibility model. The dome-shaped region of zero susceptibility (marked "D") is interpreted to represent a remanently magnetized body.

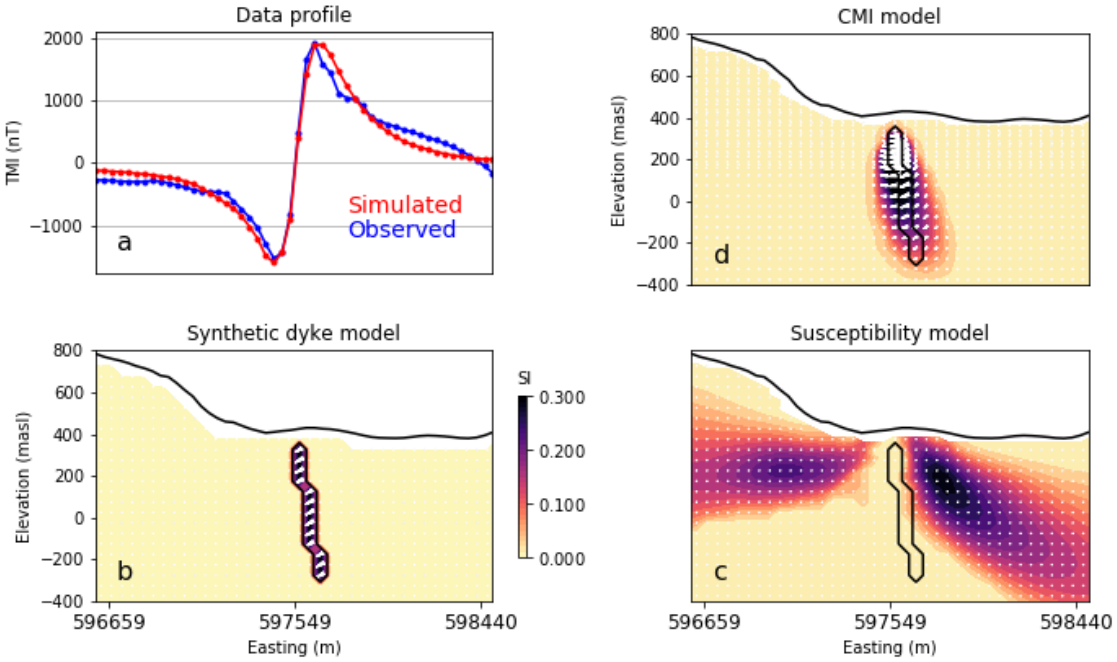

Figure 4. Numerical simulation demonstrating the effect of remanence on magnetic inversions. a) Data profile comparing the simulated and observed data over the Baker hot springs magnetic anomaly along 5401425 mN. b) The synthetic model (shown in a hypothetical E-W profile view) is made up of a steeply dipping, 50 m wide magnetic dyke with magnitude of 16 A/m and direction of I =20° and D=270°, embedded in a non-magnetic background. c) The model recovered from a susceptibility inversion (ignoring remanence) fails to recover the position and dip of the magnetized dyke. d) The Cooperative Magnetic Inversion, on the other hand, successfully images the magnetized dyke at depth.

3.2 Analytic Signal Analysis

If remanent magnetism is present in the rocks of the study area, then the map-based interpretation shown in Figure 2 may have inaccuracies. One approach for conducting map-based interpretation, in the presence of remanence, is to use the analytic signal of the magnetic field (Roest et al., 1992). Figure 5 shows the analytic signal calculated from the TMI data collected at Baker hot springs. Analytic signal is a method which assists in the determination of the geometry of magnetic source bodies regardless of the presence or absence of magnetic remanence and independent of the source body magnetization. In the analytic signal map, the dipolar anomaly is no longer present. The study area is dominated by a single source body that trends north-northeast. The analytic signal anomaly associated with this body is ~1 ¼ km long and ~½ km wide. A handful of smaller satellite bodies are found around the main body (Figure 5). Interpretation of the analytic signal map suggests a NNE-trending fault (or lithologic contact) that separates magnetic rocks to the east from weak- to non-magnetic rocks to the west. The NNE-trending structure inferred from the analytic signal map lies ~100 m west of the one inferred from the RTP anomaly map.

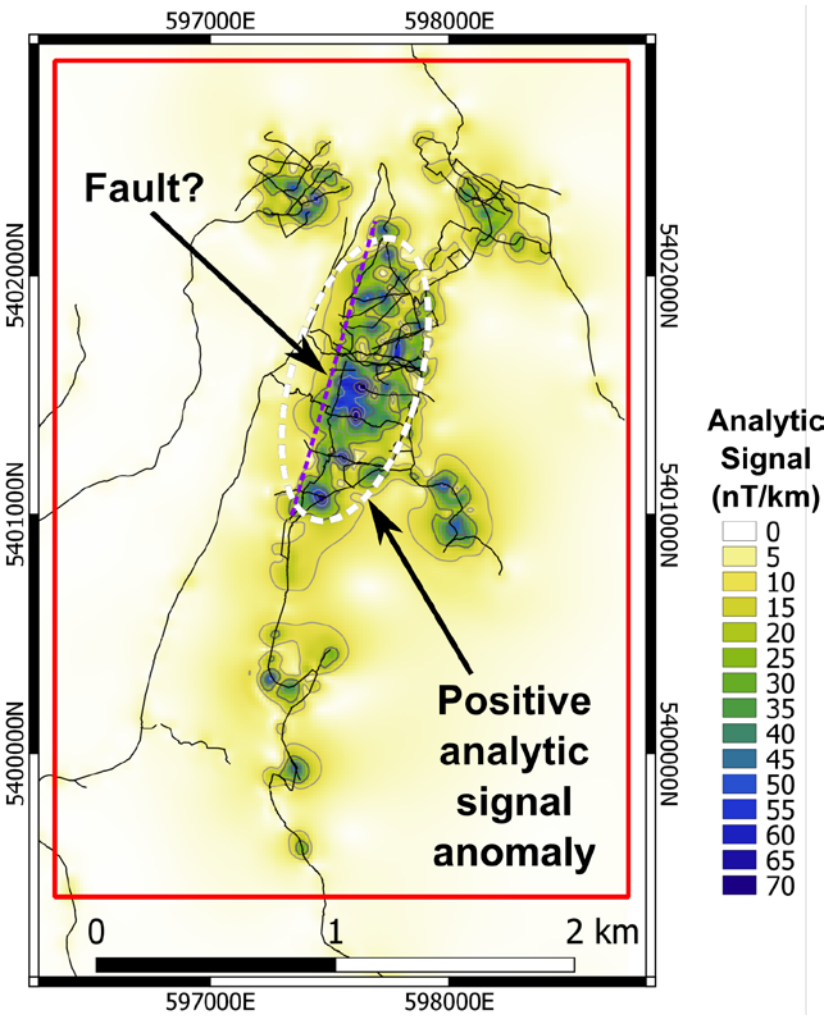

Figure 5. Analytic signal of the Total Magnetic Intensity for the Baker hot springs study area in units of nT/km. Magnetic survey lines are shown in black. Analytic signal removes the dipolar character of the dominant magnetic anomaly. Dark colours represent the possible shapes and extents of magnetic rock bodies irrespective of remanent magnetism in the subsurface. The inferred fault in this diagram is shifted west compared to the fault shown in Figure 2.

3.3 Equivalent Source Inversion Modelling

The first step in the geophysical modelling effort that accounts for remanent magnetism is equivalent source inversion modelling. The purpose of this step is to calculate magnetic amplitude data which, in turn, are inverted to generate a 3D effective susceptibility model (Li et al., 2010; Fournier, 2015). The equivalent source model is shown in Figure 6. Susceptibility values are allowed to be negative in order to fit the TMI data. Figure 7 illustrates the misfit between the observed TMI data and magnetic data calculated from the equivalent source model. Spatially, the misfit is < 1 nT over the majority of the model area. The RMS misfit calculated for the entire area is 0.3 nT.

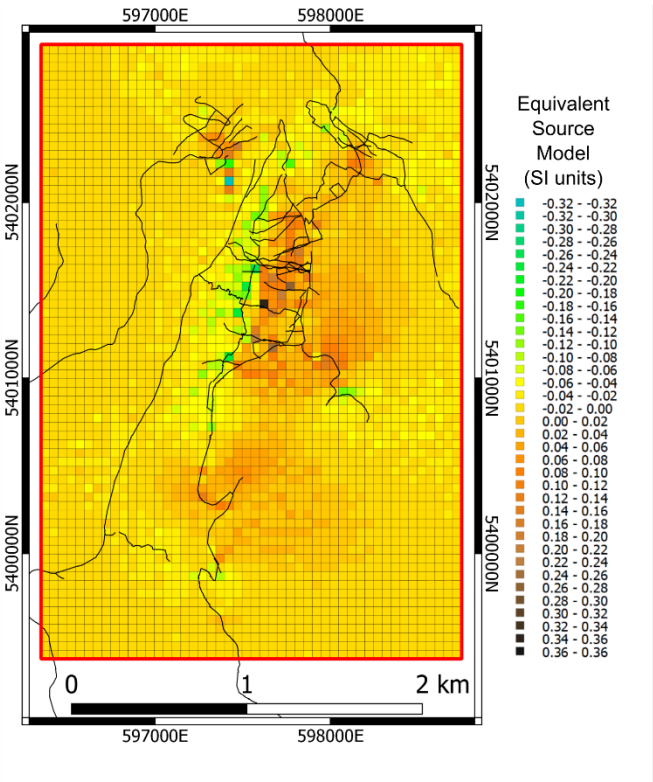

Figure 6. Equivalent source model showing the distribution of effective magnetic susceptibility in units of SI. This model consists of a thin layer and is generated solely for the purpose of calculating the magnetic amplitude data.

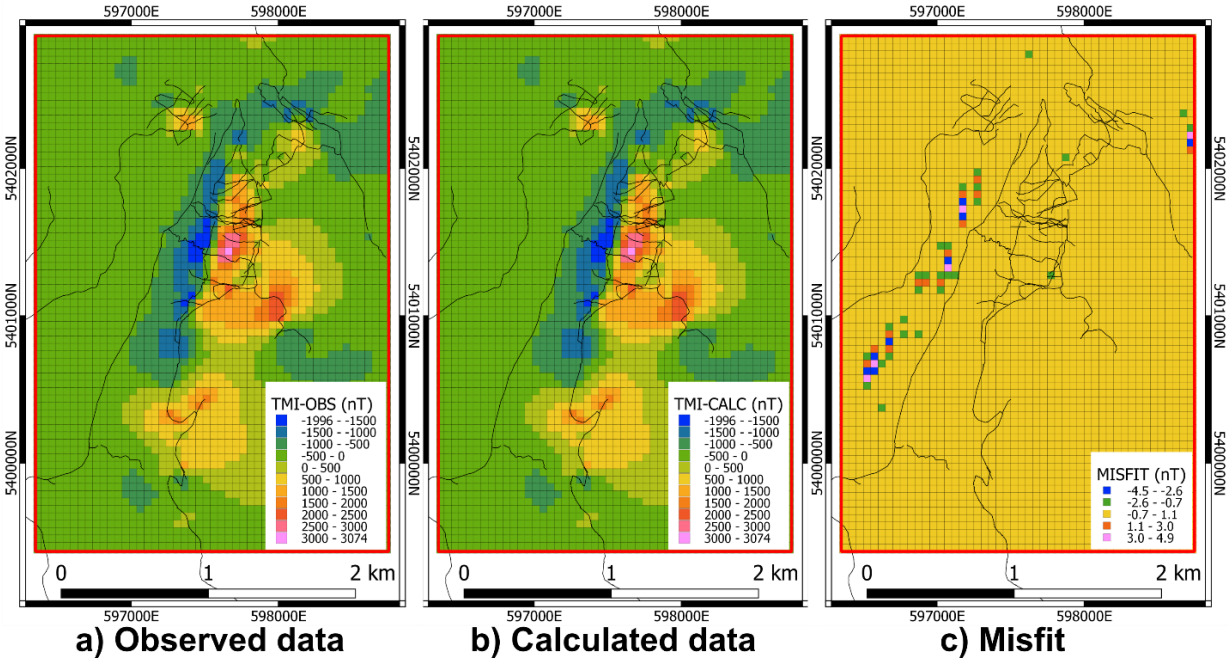

Figure 7. Maps of the a) observed TMI data, b) TMI data calculated from the equivalent source model, and c) the misfit between the two (i.e., misfit = observed – calculated). The majority of the misfit across the model area is near zero (yellow) and indicates good fit (RMS misfit = 0.3 nT). Units on the color bars are nanoTesla. Magnetic survey lines are indicated by thin black lines.

3.4 Amplitude Inversion Modelling

Inversion modelling of the magnetic amplitude data generates a 3D effective susceptibility model of the subsurface (Shearer, 2005). The values in the effective susceptibility model cannot be correlated directly with *in situ* magnetic susceptibility measurements (i.e. from hand samples). However, the relative values in an effective susceptibility model are indicative of relative variations in subsurface magnetization. A cross-section through the 3D effective susceptibility model generated in this study is shown in Figure 8. Figure 9 shows a 3D perspective view and plan view of only the regions that exhibit elevated susceptibility in the model. Figure 10 illustrates the misfit between the observed amplitude data and magnetic amplitude data calculated from the effective susceptibility model. Spatially, the misfit is < 1 nT over the majority of the model area. The RMS misfit calculated for the entire area is 0.5 nT.

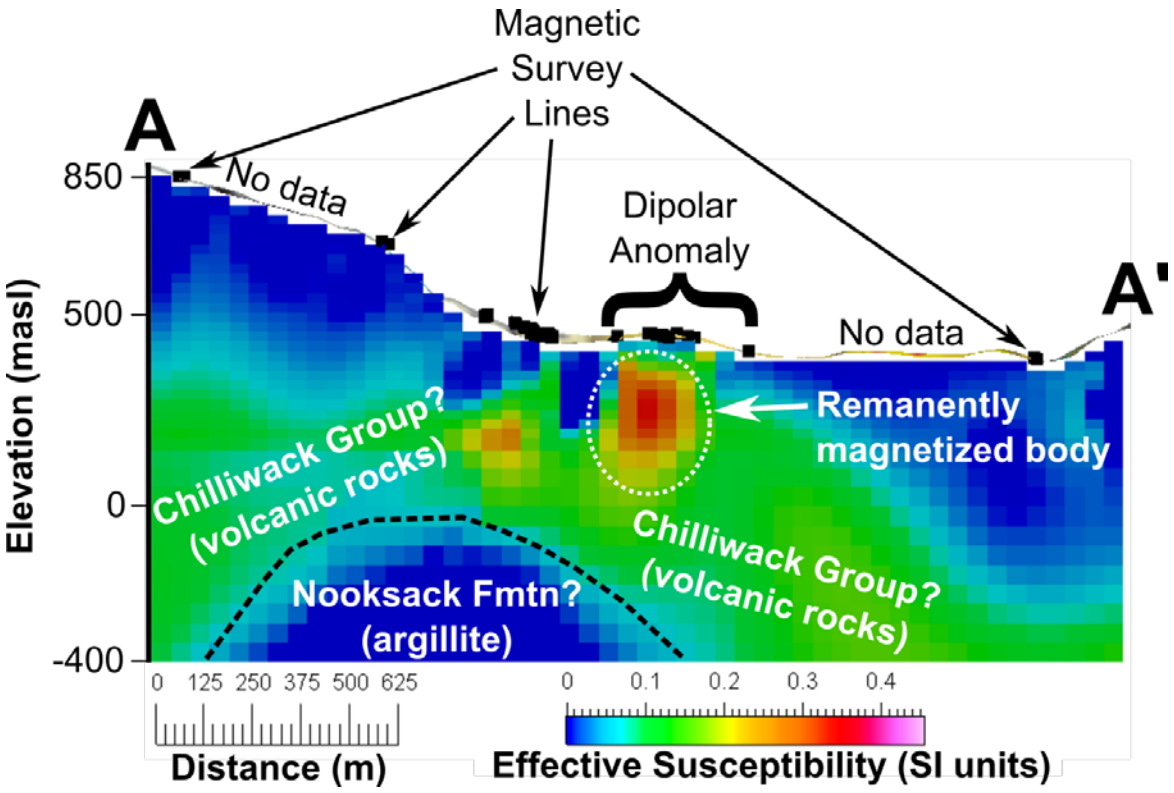

Figure 8. Section A-A' through the 3D effective susceptibility model (remanence allowed). Location of section is shown in Figure 2. Section is oriented E-W and view is to the north. Warm vs. cool colours represent high vs. low effective susceptibility, respectively. The ribbon above the model is topography. Black squares on the topography represent the locations of the magnetic survey lines. The location where the section crosses the strong dipolar RTP anomaly is labeled. The section is also annotated with a possible geologic interpretation. The black dotted line represents the geologic contact between the Chilliwack Group and Nooksack Formation rocks inferred from this effective susceptibility model. The remanently magnetized body inferred from this model is identified.

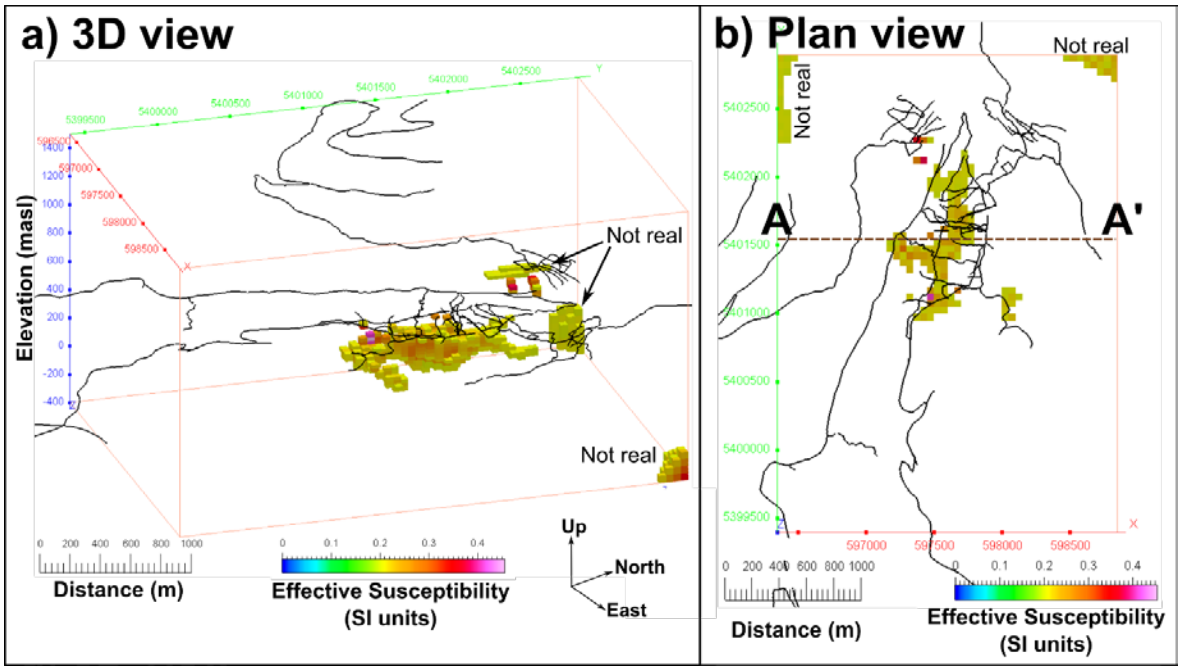

Figure 9. Effective susceptibility model shown in a) 3D perspective view to the west-northwest and b) in plan view. In order to accentuate the regions of elevated magnetization, all portions of the 3D model which have an effective susceptibility value less than 0.2 SI have been masked. Magnetic survey lines (black) are shown to illustrate where we do and do not have magnetic survey data. Regions of elevated magnetization in the NE and NW corners of the model volume are likely not real due to a lack of magnetic data. The 3D effective susceptibility model reveals a NNE-trending body of elevated magnetization. This body is irregular in shape, ~1 ¼ km long x ~200 m wide, and extends from ~25-400 m below the surface.

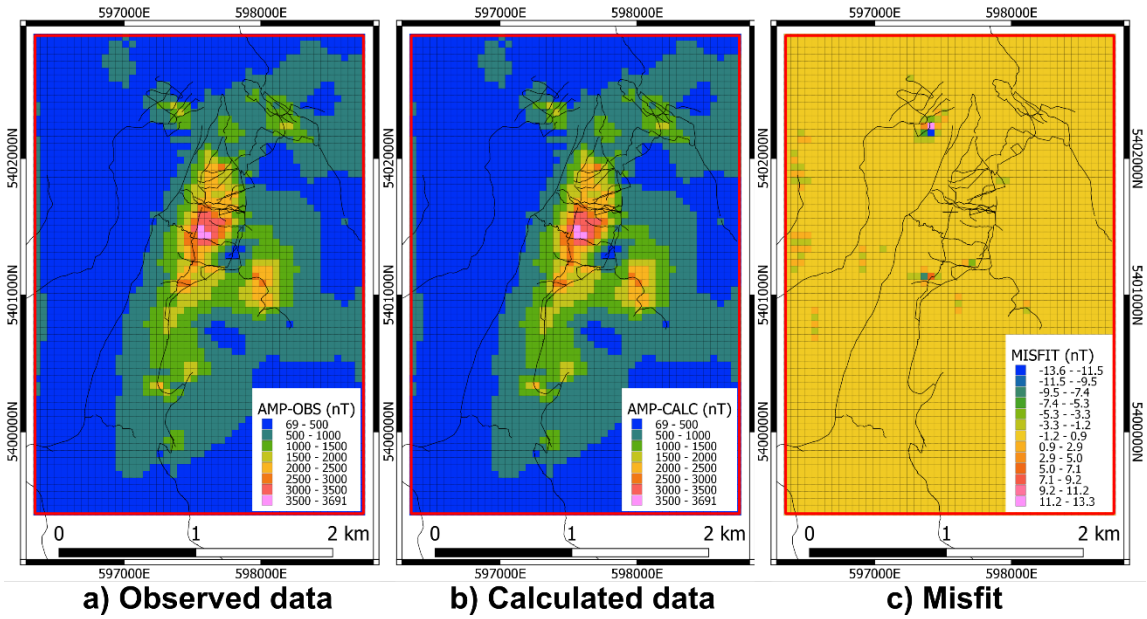

Figure 10. Maps of the a) observed Amplitude data, b) Amplitude data calculated from the effective susceptibility model, and c) the misfit between the two (i.e., misfit = observed – calculated). The majority of the misfit across the model area is near zero (yellow) and indicates good fit (RMS misfit = 0.5 nT). Units on the color bars are nanoTesla. Magnetic survey lines are indicated by thin black lines.

3.5 Cooperative Magnetic Inversion

We have so far inverted the magnetic data and recovered a 3D distribution of effective susceptibility. Differences between the susceptibility and amplitude inversion models suggest that the effect of remanence may be important (Figures 3 and 8). As a last step, we estimate the direction of magnetization to better characterize the strong dipolar anomaly observed near Baker hot springs. The Magnetic Vector Inversion of Lelièvre (2009) has proven effective in dealing with magnetic data affected by remanent magnetization. The solution is however highly non-unique, and generally yields models that are too smooth for direct geological interpretation. As a complementary strategy, Fournier (2015) proposed a cooperative magnetic inversion approach (CMI), combining the robustness of the amplitude inversion and the directionality of the MVI.

We demonstrate the capabilities of this algorithm on our synthetic dyke model, presented in Figure 4d. The CMI inversion successfully recovers the location and extent of the magnetic dyke at depth. Although wider and smoother than the true model, the inversion manages to recover the dip and magnetization orientation, greatly improving the recovery of the dipping, magnetized rock body compared to the susceptibility inversion.

Applying the same inversion strategy to the Baker hot springs data set, we recover the magnetization model presented in Figure 11. Like the amplitude inversion (Figure 8), we have recovered a continuous narrow, steeply dipping, dyke-like unit. The magnetization appears to be mainly oriented at I = 0° ± 5° and D = 280° ± 5°, which would explain the dipolar character of the anomalous magnetic field.

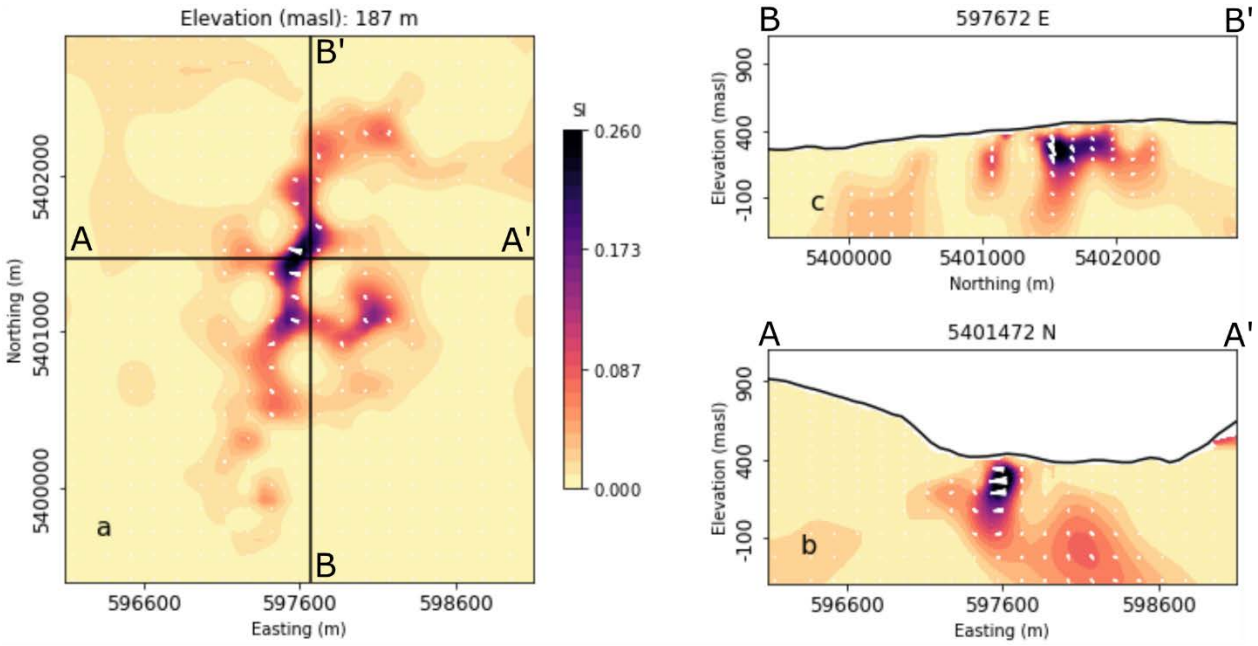

Figure 2. Sections through the recovered CMI model. White arrows indicate the magnetization direction. Dark and light colours represent high and low effective susceptibility, respectively. The region of strong magnetization is oriented at I = 0° ± 5° and D = 280° ± 5°. a) Plan map at an elevation of 187 m above sea level. b) 2D profile A-A' oriented E-W. c) 2D profile B-B' oriented N-S.

4. Discussion

The 3D effective susceptibility model generated in this study provides a geophysically robust subsurface explanation of the magnetic survey data. In addition, parts of the effective susceptibility model may be geologically reasonable. For example, the deepest rock unit in the study area stratigraphy is the Nooksack Formation, a laterally extensive, and thick (~4 km) rock unit. This unit is dominated by argillite and is expected to be weakly- to non-magnetic. These geologic observations are consistent with the susceptibility model result which places a large, thick unit with zero susceptibility at the bottom of the model (Figure 8).

Stratigraphically above this non-magnetic unit, the model shows a region with moderate and variable susceptibility (Figure 8). This type of magnetization is consistent with the Chilliwack Group rocks found above the Nooksack Formation. The Chilliwack Group rocks are mafic volcanic rocks which have undergone greenschist metamorphism to varying degrees. Rocks with this sort of geologic history would be expected to have moderate and variable magnetic susceptibility values.

The region of the 3D model exhibiting the strongest magnetization is a NNE-trending elongate, shallow body that underlies the strong, dipolar anomaly observed in the north-central portion of the magnetic map. This body is ~1 ¼ km long x ~200 m wide and extends from ~25-400 m below the surface (Figure 9). The analysis presented here suggests that this body of rock is remanently magnetized (Figure 11). These rocks could represent mafic igneous rocks intruded into the subsurface during an episode of reverse polarity. Alternatively, the zone of remanent magnetism could represent magnetite-bearing mineralization that occurred in a fault zone during a period of reverse polarity. Our magnetic modelling results are not able to discriminate between these two hypotheses.

Some portions of the 3D susceptibility model are unreliable (Figure 9). Magnetic survey data is sparse in much of the study area. Portions of the model with no magnetic survey data nearby are almost certainly incorrect (e.g. the NE and NW corners of the model). Portions of the model for which we have low confidence include regions below widely spaced magnetic survey lines (Figure 8). We have higher confidence in the model results in the north-central portion of the study area where the magnetic survey coverage is denser. Magnetic survey data that covers the entire study area with 100 – 200 m line spacing (e.g. from an airborne survey) would dramatically improve the level of confidence in the geologic interpretation of this 3D susceptibility model.

We successfully achieved low levels of misfit in the magnetic modelling effort presented here; however, geophysical modeling of any type suffers from the problem of non-uniqueness. In other words, the geophysical model result may be acceptable mathematically, but it may be incorrect geologically. One approach to reduce uncertainty and improve the model results described here would be to incorporate magnetic susceptibility measurements from the field. Such measurements could be used as an independent test of the accuracy of the 3D susceptibility model or they could serve as control points to constrain the inversion modelling process. More importantly, it would be useful to determine if the contact between the Nooksack Formation and the Chilliwack Group has a strong susceptibility contrast (as depicted in Figure 8). If there is not a strong susceptibility contrast between these two rock units, then the 3D effective susceptibility model presented here cannot be used to infer the lithologic contact between the two. The contact

between the Nooksack Formation and the Chilliwack Group is of interest because it represents an ancient thrust fault. This thrust fault may be a permeable pathway for geothermal fluids and/or offsets in this thrust fault might represent younger structures amenable to geothermal fluid flow.

5. Conclusions

This study presents results of 3D geophysical inversion modelling of magnetic data from Baker hot springs in Washington State. This area is the subject of a U.S. Department of Energy funded geothermal play fairway exploration project. Three-dimensional modelling of magnetic data is commonly used in the mineral exploration industry to identify subsurface structures and lithologic contacts that juxtapose rock units with contrasting magnetization. Geologic interpretation of magnetic model results can be hampered by the presence of rocks with remanent magnetization. Remanence arises when rocks form during episodes of Earth history when the magnetic field is reversed. We suspect that remanence is present in some of the subsurface rocks at Baker hot springs. Accordingly, we utilized a novel, multi-step inversion modelling algorithm to: 1) account for remanent magnetism and 2) deliver a more reliable 3D magnetic model. The magnetic model has reliably identified an ~1¼ km long, NNE-trending, shallow body of remanently magnetized rocks. This body may represent 1) an intrusion of reversely magnetized mafic rocks or 2) a magnetite-bearing fault zone. This rock body coincides with the location of the Baker hot springs; the margins of this body or the fault structures within it are likely responsible for providing the permeability that gives rise to the hot springs. The 3D magnetic model also appears to be broadly consistent with the larger-scale geology of the study area. Specifically, the magnetic model displays a thick unit of non-magnetic rocks underlying a unit of moderate and variable magnetization. This is consistent with the geologic understanding of the area which comprises non-magnetic, argillite-dominated, Nooksack Formation underlying greenschist facies mafic volcanic rocks of the Chilliwack Group. Due to the sparse magnetic survey coverage, the 3D magnetic model is unreliable in some areas and questionable in others. Geologic interpretation of the Baker hot springs area would be greatly improved with complete magnetic survey data covering the entire study area (e.g. an airborne magnetic survey) coupled with numerous measurements of bedrock magnetic susceptibility to constrain the 3D magnetic inversion modelling.

REFERENCES

Cockett, R., Kang, S., Heagy, L.J., Pidlisecky, A., and Oldenburg, D.W. “SimPEG: An open source framework for simulation and gradient based parameter estimation in geophysical applications.” Computers & Geosciences, 85, (2015), 142-154.

Fournier, D. “A Cooperative Magnetic Inversion Method with Lp-norm Regularization.” *MSc thesis*, University of British Columbia, Vancouver, British Columbia, (2015), 155 pages.

Lelièvre, P.G. “Integrating geological and geophysical data through advanced constrained inversion.” *Phd thesis*, The University of British Columbia, Vancouver, British Columbia, (2009), 177 pages.

Li, Y., Nabighian, M.N., and Oldenburg, D. “Using and equivalent source with positivity for low-latitude reduction to the pole without striation.” *Geophysics*, 79, (2014), J81–J90.

Li, Y. and Oldenburg, D.W. “3-D inversion of magnetic data.” *Geophysics*, 61, (1996), 394-408.

Li, Y. and Oldenburg, D.W. “Rapid construction of equivalent sources using wavelets.” *Geophysics*, 75, (2010), L51-L59.

Li, Y., Shearer, S.E., Haney, M.M., and Dannemiller, N. “Comprehensive approaches to 3D inversion of magnetic data affected by remanent magnetization.” *Geophysics*, 75, (2010), L1–L11.

Nabighian, M.N. “The analytic signal of two-dimensional magnetic bodies with polygonal cross-section.” Geophysics, 37, (1972), 507–517.

Norman, D.K., Forson, C., Czajkowski, J.L., Swyer, M.W., Cladouhos, T.T., Shcmalzle, G.M., and Davatzes, N. “Geothermal Play-Fairway Analysis of Washington State Prospects: Phase 1 Technical Report.” Washington Division of Geology and Earth Resources, (2015), 101 pages.

Roest, W.R., Verhoef, J., and Pilkington, M. “Magnetic interpretation using the 3-D analytic signal.” *Geophysics*, 57, (1992), 116-125.

Schermerhorn, W.D., Ritzinger, B., Anderson, M., Witter, J., Glen, J., Forson, C., Stelling, P., and Fournier, D. “Geothermal Exploration of Mount Baker Hot Springs Through Ground-Based Magnetic and Gravity Surveys.” *Proceedings, 42nd Workshop on Geothermal Reservoior Enginnering*, Stanford University, Stanford, California, (2017), 13 pages.

Shearer, S. “Three-dimensional inversion of magnetic data in the presence of remanent magnetization.” *Master’s thesis*, Colorado School of Mines, Golden, Colorado, (2005).

Tabor, R.W., Haugerud, R.A., Hildreth, W., and Brown, E.H. “Geologic Map of the Mount Baker 30- by 60-Minute Quadrangle, Washington.” Geologic Investigations Series I-2660, U.S. Geological Survey, (2003).